Available online at www.sciencedirect.com
ScienceDirect
Scripta Materialia 56 (2007) 685–688
Scripta MATERIALIA
www.actamat-journals.com

# Mechanical enhancement of carbon fiber/epoxy composites by graphite nanoplatelet reinforcement

J. Cho, J.Y. Chen and I.M. Daniel*

*Center for Intelligent Processing of Composites, McCormick School of Engineering and Applied Science, Northwestern University, Evanston, IL 60208, USA*

Received 6 October 2006; revised 21 December 2006; accepted 22 December 2006
Available online 23 January 2007

The epoxy matrix in carbon fiber/epoxy composites was modified with graphite nanoplatelets to improve their mechanical properties. Graphite nanoparticles were mixed and dispersed in the epoxy matrix by sonication, followed by a vacuum assisted wet lay-up process. The composites reinforced with nanoparticles showed enhanced compressive strength and in-plane shear properties. A simple analytical model was used to predict the longitudinal compressive strength, which was in good agreement with experimental results.


*Keywords:* Graphite nanoplatelets; Composite; Compressive strength; In-plane shear properties; Wet lay-up

Continuous fiber/epoxy composites have been widely used for structural applications due to their excellent mechanical properties. However, their matrix-dominant properties, such as in-plane and interlaminar shear properties, are much weaker than their fiber-dominated properties, thus limiting the benefits of conventional composites. In addition, it is known that composites exhibit lower longitudinal compressive strength, a matrix-dominated property, than tensile strength [1]. Thus, it is desirable to improve all matrix-dominated properties to enhance the potential of structural applications of composites.

Several attempts have been made recently to achieve this goal by reinforcing the matrix with nanoparticles [2–4], or by introducing nanoparticle/epoxy films between composite plies [5]. It was reported that the interlaminar shear strength of glass fiber/epoxy composites is improved by 20% with the introduction of 0.3 wt.% amino-functionalized multiwall carbon nanotubes [2]; the compressive strength of carbon fiber/epoxy composites is enhanced by 10–15% with 10 wt.% of cup-stacked type carbon nanofibers [3]; and the compressive strength of glass fiber/vinyl ester composites is increased by 16% with 3 wt.% of clay nanoparticles [4]. In Ref. [5], it was shown that inserting 3501-6 epoxy films with 0.2 wt.% functionalized single-wall carbon nanotubes between AS4/3501-6 plies increases the interlaminar shear strength of the composite by 1.7%. This very moderate improvement was attributed to the nonuniform dispersion of the nanotubes. Based on these investigations [2–5], it was concluded that the matrix-dominated properties of fiber/polymer matrix composites can be improved using nanoparticles, with the extent of the improvement depending on the processing method and the type, surface condition, concentration and dispersion of the nanoparticles.

In this study, the longitudinal compressive strength and in-plane shear properties of carbon fiber/epoxy composites with graphite nanoplatelets were investigated. The epoxy matrix was reinforced with particle loadings of 3 and 5 wt.%. In addition, an analytical model was investigated of the effect of matrix reinforcement on the compressive strength of the composite.

The matrix material used in this study was a three-part epoxy system manufactured by Vantico (currently, Huntsman). This system consists of epoxy resin DGEBA (GY6010), anhydride hardener (Aradur 917) and accelerator (DY070), which are typically mixed in the ratio of 100:90:1 by weight, respectively. The graphite particles were obtained from Asbury Carbons (Grade 4827). The particles are synthetic graphite of over 98% purity and density of approximately 2.25 g $cc^{-1}$. The

* Corresponding author. Tel.: +1 847 491 5649; fax: +1 847 491 5227; e-mail: imdaniel@northwestern.edu

1359-6462/$ - see front matter © 2007 Acta Materialia Inc. Published by Elsevier Ltd. All rights reserved.
doi:10.1016/j.scriptamat.2006.12.038

typically disk-like graphite particles were estimated to range between 0.5 and 5 μm in mean diameter and 100–200 nm in thickness based on scanning electron microscope (SEM) images (Fig. 1). A unidirectional carbon fiber perform, with the carbon fiber tows held by transverse glass fiber yarns, was used. The perform density was 1.8 g $cm^{-3}$.

A weighed amount of the graphite nanoparticles was prepared based on the weight fraction of the particles to the total weight of the epoxy and graphite mixture. The as-received nanoparticles were dispersed in acetone by ultrasonic sonication (Cole-Parmer 500-Watt Ultrasonic Processor) for 1 h. After sonication, the mixture of DGEBA, particles and acetone was prepared and stirred with a magnetic stirrer on a hot-plate until the DGEBA was completely dissolved in the acetone at 75 °C, and subsequently sonicated for 30 min. After removing all acetone from the mixture, the hardener was added and the mixture stirred on the hot-plate at 50 °C for 0.5–1 h. Subsequently, the accelerator was added and the mixture stirred on the hot-plate at 50 °C for 0.5 h with slow agitation, followed by degassing for 0.5–1 h.

Dry carbon fiber preforms and prepared resin mixture with or without nanoparticles were processed by vacuum assisted wet lay-up. In this processing method, the fiber perform layers were successively impregnated by pouring and evenly spreading a metered volume of the resin and stacked. The composite laminate was then cured in a hot-press at 149 °C for 1 h at a heating rate of 2.2 °C $min^{-1}$, under an applied pressure of 2.07 MPa. The excess resin was squeezed out of the composite by vacuum of 100 kPa. By this process, composite laminates were produced with a fiber volume ratio of 0.55 (±3%).

Compression tests were conducted with a specially designed fixture, NU fixture [1,6], at a crosshead rate of 0.0762 mm $min^{-1}$. In-plane shear properties were measured by the 10° off-axis test method [7,8]. All tests were carried out in a servohydraulic testing machine while recording load and deformation data on a computer.

The results shown in Table 1 clearly indicate that the compressive strength and in-plane shear properties of the composite are enhanced with the nanoparticle reinforced epoxy matrix. Compared with the properties of the unreinforced neat resin composite, the in-plane shear modulus is enhanced by 7 and 18%, the shear strength is improved by 6 and 11%, and the longitudinal compressive strength is increased by 10 and 16% with the addition of 3 and 5 wt.% of nanoparticles, respectively.

**Table 1.** Results of compressive and in-plane shear property tests

| Nanoparticle content (wt.%) | In-plane shear | | Compressive strength (MPa) |
|---|---|---|---|
| | Modulus (GPa) | Strength (MPa) | |
| 0 | 5.8 (< ± 1%) | 374 (±5%) | 551 (±3%) |
| 3 | 6.2 (< ± 1%) | 399 (±3%) | 608 (±3%) |
| 5 | 6.8 (< ± 1%) | 416 (±2%) | 638 (±2%) |

The enhanced in-plane shear modulus of the hybrid composite can be explained by the increased shear modulus of the nanocomposite matrix. The shear stress–strain curves of the nanocomposites and the neat resin are shown in Figure 2. They were obtained by the Iosipescu shear test (ASTM D5379). It is clearly seen from Figure 2 that the shear modulus increases as the particle loading increases. However, the shear strength of the nanocomposite exhibits little improvement with the particle loading increase. Published papers show a noticeable decrease in tensile and flexural strength with increased particle loading [9–11]. However, unlike the tensile stress failures, in the case of shear loading seen in Figure 2, the nanocomposites exhibit pronounced nonlinear behavior with large strains to failure. Furthermore, the shear strength of the nanocomposites is not significantly lower than that of the neat resin.

Under in-plane shear loading, the fiber reinforced composite can be analyzed as a series model with constant average shear stress in the fibers and matrix [1]. The matrix-dominated shear strength, $F_{12}$, can be related to the shear strength of the neat or nanocomposite matrix, $F_{ms}$, and the shear stress concentration factor as

$$F_{12} \approx \frac{F_{ms}}{k_\tau}. \quad (1)$$

This stress concentration factor, $k_\tau$, is expressed as

$$k_\tau = \frac{1 - V_f(1 - G_m/G_f)}{1 - (4V_f/\pi)^{1/2}(1 - G_m/G_f)}, \quad (2)$$

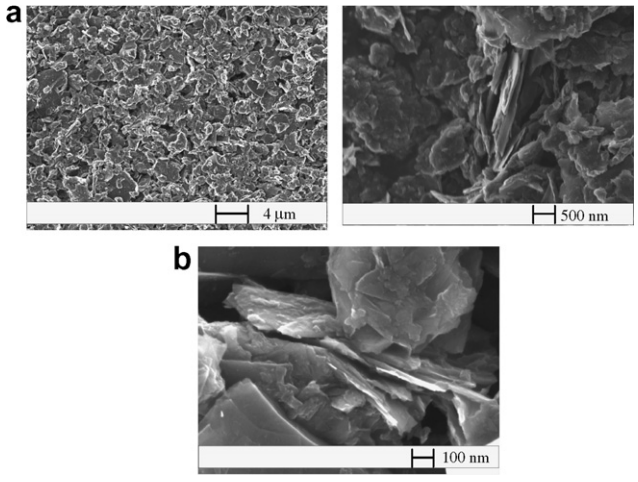


**Figure 1.** SEM images of graphite nanoplatelets: (a) before sonication; (b) after sonication.

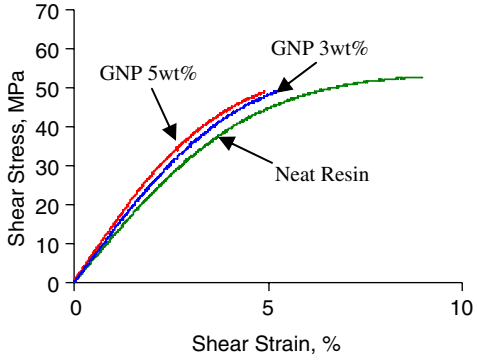


**Figure 2.** Shear stress–strain curve of nanocomposite with various nanoparticle loadings.

where $V_f$ is fiber volume ratio and $G_m$ and $G_f$ are shear moduli of the matrix and fiber, respectively. As shown in Figure 3, the stress concentration factor decreases as the particle loading increases. Thus, the increase of the in-plane shear strength of the fiber reinforced composite can be explained by the stress concentration decrease and the small change in nanocomposite shear strength with particle loading.

Rosen's analysis [12] of compressive failure of continuous fiber composites associated compressive strength with microbuckling of the fibers within the matrix. For composites with a high fiber volume fraction, he proposed that the compressive strength is directly proportional to the shear modulus of the matrix and inversely proportional to the matrix volume fraction. However, it was found that Rosen's compressive strength prediction overestimates experimentally measured data, due to pre-existing fiber misalignment and nonlinear nature of the matrix [13–15].

In this study, a simple model [1], taking into account initial fiber misalignment and nonlinear mechanical behavior of the matrix, was used to predict the compressive strength enhanced by the nanoparticles. In the model, it is assumed that there is an initial fiber misalignment $\varphi$ with respect to the loading direction. After loading, there is additional fiber rotation due to in-plane shear strain, $\gamma_{12}$. For small $\varphi$ and $\gamma_{12}$, the applied axial stress $\sigma_c$ is obtained as

$$\sigma_c \cong \frac{-\tau_{12}}{(\varphi + \gamma_{12})}, \tag{3}$$

where $\tau_{12}$ is the in-plane shear stress. To obtain a maximum $\sigma_c$, the derivative of $\sigma_c$ with respect to $\gamma_{12}$ must be equal to zero, which results in

$$\frac{\partial \tau_{12}}{\partial \gamma_{12}} = \frac{\tau_{12}}{(\varphi + \gamma_{12})}. \tag{4}$$

By obtaining the $\tau_{12}$ and $\gamma_{12}$ values satisfying Eq. (4) from the experimentally obtained in-plane shear stress–stain curves and substituting in Eq. (3), the compressive strength of the composites can be calculated.

The composite laminate fabricated in this study possesses crimps in the thickness direction due to the glass fiber yarns holding the carbon fibers. Locally (but distributed in the composite), these crimps cause initial fiber misalignment, and consequently play a dominant role in compressive failure [16]. Figure 4 shows the compressive failure through the thickness direction due to the fiber misalignment caused by the crimps.

Initial fiber misalignment was measured graphically at different sites of the specimens in the compression tests, and an effective fiber misalignment of 4.0° (±0.2°) was determined by averaging the measurements. It must be mentioned here that, since unidirectional composites are considered as transversely isotropic materials, throughout the thickness, fiber misalignment can be treated like in-plane misalignment using in-plane shear properties in the analysis. Thus, in this study, the effective misalignment angle determined was used in Eq. (3) and subsequently the $\tau_{12}$ and $\gamma_{12}$ values satisfying Eq. (4) were obtained from the experimentally measured in-plane shear stress–stain curves in Figure 5. It is seen in Figure 6 that the calculated compressive strengths from this model compare fairly well with experimental results. Also, as shown in Figure 6, it is seen that, in order to improve the compressive strength further, the fiber misalignment must be reduced.

In this study, we have demonstrated that in-plane shear modulus and strength and compressive strength of carbon fiber/epoxy composites are enhanced by reinforcing the matrix with graphite nanoplatelets. It was shown that the increase of the in-plane shear strength of the fiber reinforced composite with particle concentration may be attributed to the increase in shear

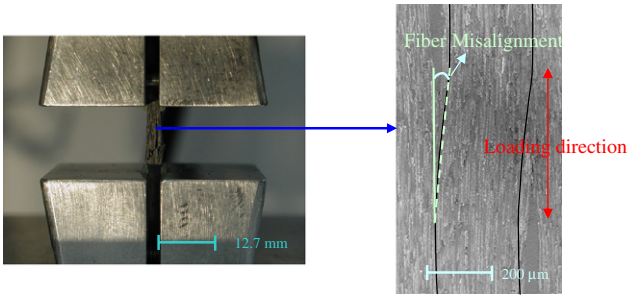


**Figure 4.** Compressive failure and fiber misalignment.

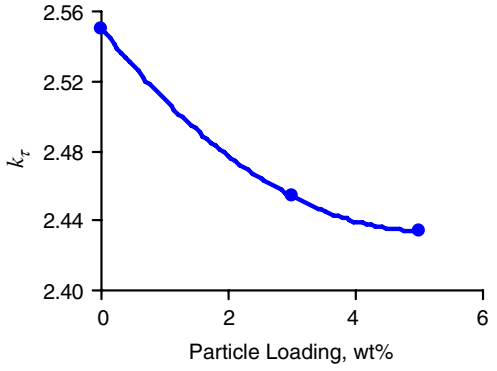


**Figure 3.** Shear stress concentration factor in fiber-reinforced composite.

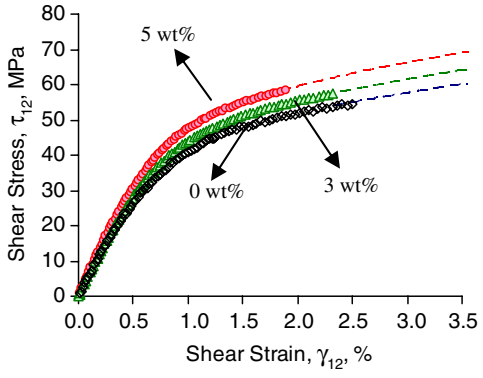


**Figure 5.** In-plane shear stress–strain curves for different nanoparticle contents (dashed lines extended from the experimentally obtained curves using $\tau_{12} = k(\gamma_{12})^n$).

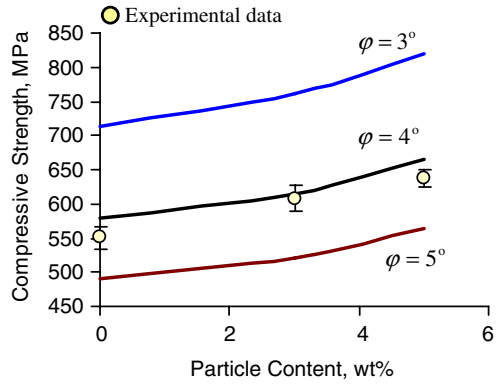


**Figure 6.** Comparison of measured and predicted compressive strengths for three values of fiber misalignment.

modulus of the nanocomposite matrix and the resulting decrease in the shear stress concentration factor. It was also shown using a model that the compressive strength improvement results from the enhanced in-plane shear properties by the nanoparticles, and that this strength can be further improved by reducing the initial fiber misalignment.

We gratefully acknowledge the grant support from the NASA University Research, Engineering and Technology Institute on Bio Inspired Materials (BIMat) under award No. NCC-1-02037.

[1] I.M. Daniel, O. Ishai, Engineering Mechanics of Composite Materials, 2nd ed., Oxford University Press, Inc., New York, 2006.
[2] F.H. Gojny, M.H.G. Wichmann, B. Fiedler, W. Bauhofer, K. Schulte, Compos. Part A 36 (2005) 1525.
[3] Y. Iwahori, S. Ishiwata, T. Sumizawa, T. Ishikawa, Compos. Part A 36 (2005) 1430.
[4] A.K. Subramaniyan, C.T. Sun, Compos. Part A 37 (2006) 2257.
[5] K. Adhikari, P. Hubert, B. Simard, in: 47th AIAA/ASME/ASCE/AHS/ASC Structures, Structural Dynamics, and Materials Conference, Newport, Rhode Island, 2006, pp. AIAA 2006.
[6] H.M. Hsiao, I.M. Daniel, S.C. Wooh, J. Compos. Mater. 29 (1995) 1789.
[7] I.M. Daniel, T. Liber, Lamination Residual Stresses in Fiber Composites, NASA Glen Research Center, Cleveland, OH, 1975.
[8] C.C. Chamis, J.H. Sinclair, Exp. Mech. 17 (1977) 339.
[9] J. Li, J.K. Kim, M.L. Sham, Scripta Mater. 53 (2005) 235.
[10] Y.X. Pan, Z.Z. Yu, Y.C. Ou, G.H. Hu, J. Polym. Sci. Part B Poly. Phys. 38 (2000) 1626.
[11] A. Yasmin, J.J. Luo, I.M. Daniel, Compos. Sci. Technol. 66 (2006) 1182.
[12] B.W. Rosen, in: Fiber Composite Materials, ASM, Materials Park, OH, 1965.
[13] I.M. Daniel, H.M. Hsiao, S.C. Wooh, Compos. Part B 27 (1996) 543.
[14] J.G. Haberle, F.L. Matthews, J. Compos. Mater. 28 (1994) 1618.
[15] C.T. Sun, A.W. Jun, Compos. Sci. Technol. 52 (1994) 577.
[16] H.M. Hsiao, I.M. Daniel, Compos. Sci. Technol. 56 (1996) 581.